JOURNAL OF MATERIALS SCIENCE **35** (2000) 599–607

In situ mechanical testing of dry and hydrated breadcrumb in the environmental scanning electron microscope (ESEM)

D. J. STOKES, A. M. DONALD*
Polymers & Colloids, Department of Physics, University of Cambridge, Cavendish Laboratory, Madingley Road, Cambridge, CB3 0HE, England, UK
E-mail: amd3@phy.cam.ac.uk

The environmental scanning electron microscope (ESEM) has the ability to image both dry and hydrated materials, without the need for a conductive coating, unlike conventional SEM. This presents a unique opportunity to explore the structure and dynamic mechanical characteristics of food systems, including those in a moist state. We have developed a technique in which quantitative stress-strain relationships can be obtained whilst allowing simultaneous imaging, by ESEM, of the mechanical response of a sample. The results of *in situ* compression tests on dry and hydrated wheat flour breadcrumbs are presented and discussed. It was found that a maximum in the critical fracture stress occurred at intermediate moisture content (∼16%). ESEM micrographs demonstrate the differences in mechanical behaviour at three different moisture contents (nominally dry, 16% and 30%). Our findings suggest that 'voids' in cell walls, along with discontinuities between starch granules and gluten in the crumb, play an important role in fracture initiation. Further evidence shows that voids may be bridged by 'struts' and 'strings' of matrix material, which may be factors in the control of fracture propagation.

1. Introduction

Breadcrumb is an example of a manufactured cellular solid, consisting of partially gelatinized starch granules in a gluten matrix, supporting cells formed by escaping gases during baking [1]. The structure is that of an open cell foam, whose mechanical properties largely depend on the composition of the crumb, such as moisture content, cell size and shape and cell wall thickness. The precise nature of the cell walls is governed by the relative proportions of ingredients and on the processing and cooking conditions. A crisp texture is associated with a low moisture content and low water activity level, when the starch/gluten matrix is in a glassy state. Increasing the water content of low moisture foods tends to lower the glass transition temperature T_g of the matrix, eventually leading to loss of crispness via a plasticizing effect.

Breadcrumb coated foods, such as fish, cheese, fruits, meat, poultry, vegetables and sea foods, are a fast-growing food category [2]. Such coatings, usually based on cereal flour, help to provide and protect flavour, texture and appearance, and may also be needed to help prevent oxidation, limit oil transfer, give freeze-thaw stability and extend shelf life [3]. Given that a breaded food product (for example breadcrumb-coated chicken) has a low moisture content and low water activity on the exterior and a high moisture content and high water activity on the interior, there is a driving force to equilibrate the widely differing water activity levels during storage, resulting in a soft and soggy crumb coating. It is usually possible to re-crisp the coating during deep fat frying or oven baking, although microwave cooking does not provide sufficient dehydration in the majority of cases [4]. It is therefore of interest to explore the microstructural changes that occur in breadcrumb as function of moisture content. Although several instrumental and sensory techniques are available for the analysis of parameters such as stress, strain, elastic modulus and textural attributes, it has not previously been possible to study bulk properties using a real-time visual technique.

Various instrumental studies have shown [5–8] that cellular cereal products have a tendency to be brittle and fragile at very low moisture content, with their resistance to fracture increasing significantly up to around 9–10% moisture. Beyond this, plasticisation begins to reduce the stiffness of the material rapidly, as the glass transition temperature T_g is lowered. Our studies are in broad agreement with these findings, as will be demonstrated. It was found that the dry crumb exhibited brittle behaviour, but that the resistance to fracture increased up to about 16% moisture content. At a higher moisture level, arbitrarily chosen to be 30% in this study, the crumb was plasticised and had little resistance to deformation.

* Author to whom all correspondence should be addressed.

The aim of this work was to develop a complementary technique in which quantitative stress-strain data are linked with simultaneous imaging by electron microscopy, and then to apply the methodology to a specific system. A specially designed straining stage was therefore used, so that dynamic mechanical tests could be carried out within the specimen chamber of an environmental scanning electron microscope (ESEM). The technique was applied to breadcrumb in an attempt to gain insight into the influence of moisture content on the structural and mechanical characteristics of this material, and the results are presented by means of graphical data and the corresponding ESEM images.

2. Background to ESEM

The ESEM is able to image uncoated and hydrated samples by means of a differential pumping system, and gaseous secondary electron detector [9]. The differential pumping system, illustrated in Fig. 1, enables the electron gun and upper parts of the column to be held at high vacuum (10^{-7} torr), whilst the level of vacuum becomes progressively lower further down the column. Pressure limiting apertures allow the electron beam to pass through, but minimize the leakage of gases between zones pumped at different rates. Within the specimen chamber, pressures of up to 20 torr can be maintained [9]. The presence of water vapour, or other imaging gas, causes some scattering of the primary electron beam. Because the pressure is still low enough to prevent multiple scattering a sharp probe remains, superimposed on an additional large, flat 'skirt'. The signal-to-background ratio remains high, and it is possible to obtain images with a resolution of a few nanometres, depending on sample characteristics [9]. Hydrated specimens can be stabilized by means of careful control of sample temperature and chamber pressure, in order to maintain a saturated vapour pressure of water above the sample. The saturated vapour pressure curve of water in Fig. 2 indicates the criteria needed for stabilization of the sample. These conditions are particularly suited to

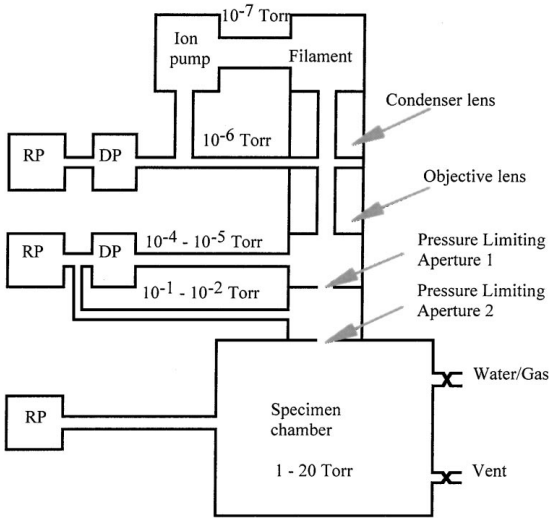

Figure 1 Schematic diagram of the column of the ESEM, showing the differential pumping zones and pressure limiting apertures (not to scale). RP = rotary pump, DP = diffusion pump.

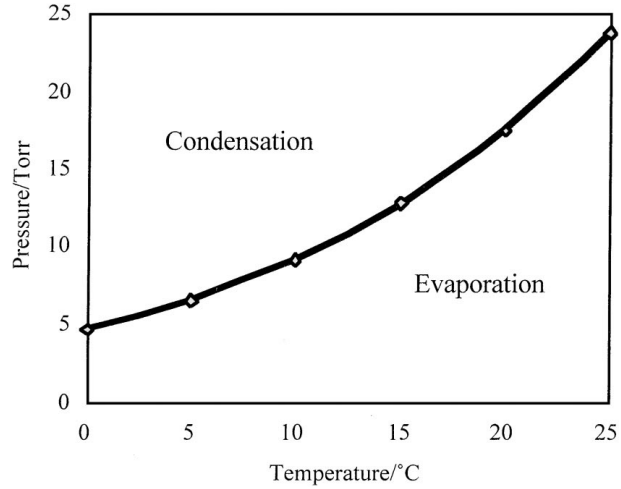

Figure 2 The saturated vapour pressure curve of water, showing the conditions necessary for stabilization of water-containing samples. Appropriate changes to the temperature of the sample or the pressure within the specimen chamber lead to condensation or evaporation of water.

the observation of organic/biological specimens in their natural state, especially as many such samples contain water (although care is needed in order to avoid damage to the sample by the irradiating electron beam). Specimens may also be deliberately hydrated or dehydrated *in situ*, by shifting conditions in favour of condensation or evaporation of water. This can be achieved by adjusting temperature and/or pressure, in accordance with Fig. 2. Particular care is needed to ensure that hydration or dehydration of samples is minimized during the initial pumpdown, when air in the chamber is systematically replaced by water vapour. With this in mind, an optimized pumpdown sequence has been developed [10].

An equally important feature of the ESEM, is the gaseous secondary electron detector (GSED), or environmental secondary detector (ESD), which replace the customary Everhart-Thornley and other solid state backscattered electron detectors used in conventional SEM. The GSED (or ESD) actually relies on the presence of the gas between itself and the sample, as the gas acts as a means of amplifying the signal generated by secondary electrons. The amplification of secondary electrons arises via a gas cascade [11, 12], initiated as the emitted secondary electrons collide with and ionize gas molecules on their way to the positively biased detector. Further electrons are produced as a result, and these will also undergo ionizing collisions, thus propagating the cascade and amplifying the signal, as shown in Fig. 3. A by-product of the gas cascade is the production of positive ions that fall towards the sample surface, thereby helping to neutralize negative charge build-up. Conveniently, water vapour has been found to possess the most efficient cascade properties of any gas tested [13].

3. Experimental

3.1. Sample preparation

Loaves of bread were prepared to a standard recipe, using 300 g breadmaking wheat flour, 6 g salt, 3 g flour improver (containing DATEM, amylase and ascorbic

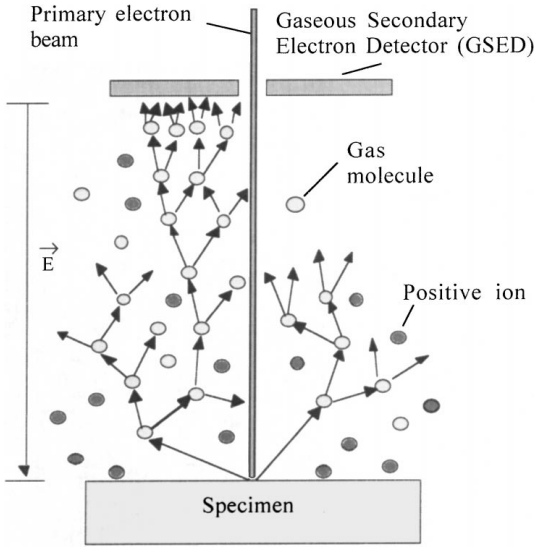

Figure 3 A simplified schematic diagram of the gaseous secondary electron detector (GSED) in the ESEM. The primary electron beam impinges on the sample, leading to the production of backscattered (not shown) and secondary electrons. The positively biased detector accelerates secondary electrons through the sample-to-detector gap, colliding with and ionizing gas molecules on their way, initiating a cascade of further electrons and amplifying the signal. Positively charged ions fall towards the sample surface, helping to neutralize negative charge build-up.

acid) 180.5 g tap water and 7.5 g wet, block yeast, and baked for 20 minutes in a deck oven at 200°C. After cooling overnight, the loaves were sliced to a thickness of ∼1 cm and dried in a domestic fan oven for 5 minutes at 102°C. Each slice was further cut into 1 cm cubes and dried for 3 hours at 102°C, to give nominally dry crumb samples. Final preparation involved cutting each cube with a scalpel blade to give cuboids with typical dimensions of 5 mm × 5 mm × 8 mm: each was accurately measured with Vernier calipers prior to compression testing.

3.2. Mechanical testing

Mechanical tests were performed using a specially designed straining stage with a heat exchanger, built by Oxford Instruments, adapted to include a Peltier chip for temperature variation to permit the controlled hydration of samples, as described earlier. The stage may be operated in either tension or compression, as required. A schematic diagram of the straining stage is shown in Fig. 4. A 25 kgf load cell was used, and the load versus deformation data was collected at a rate of 2.5 readings per second. This data was fed to a computer where it was converted to stress-strain information, based on the initial cross-sectional area and gauge length of the sample, and cross head speed. The cross head speed was 10 μm per second in all cases. If it is assumed that the cross-sectional area of the sample being tested does not change appreciably, then it is convenient to use the 'engineering' stress and strain, avoiding the use of a correction factor for cross-sectional area expansion during mechanical testing [14]. The engineering stress σ_E and strain ε_E are defined as follows:

$$\sigma_E = F/A_0 \quad (1)$$

$$\varepsilon_E = \Delta l/l_0 \quad (2)$$

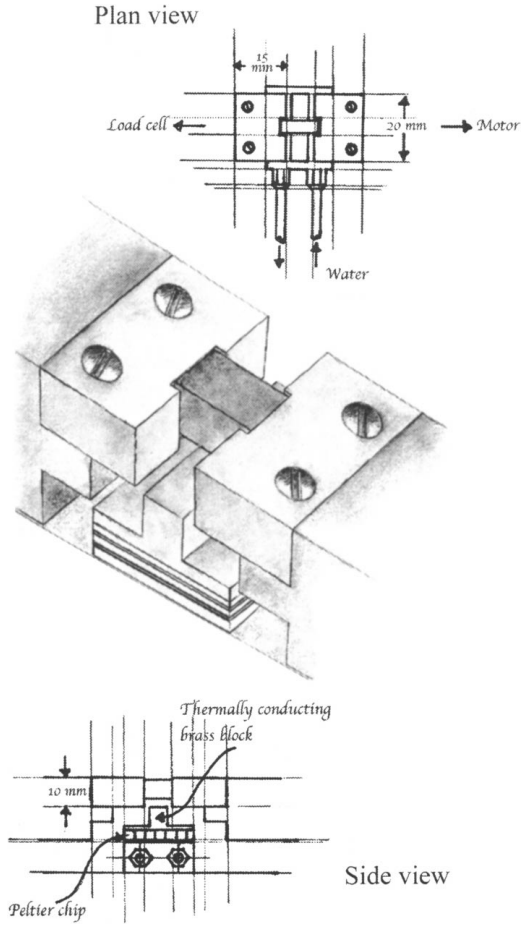

Figure 4 Diagrams of the custom built straining stage for testing samples within the specimen chamber of the ESEM. The water-chilled Peltier chip enables cooling of samples which, together with an appropriate chamber pressure (see Fig. 2), allows samples to be maintained in a hydrated state.

where F = force, A_0 = initial cross-sectional area of the sample, l_0 = initial length and Δl = change in length of the sample.

In the first instance, crumbs at various moisture contents were compression tested using the straining stage described above, but with the stage operated outside the microscope. This was done to ensure that the data produced did not contain artefacts due to changes in moisture content of samples in the environment of the microscope chamber. Samples for these control experiments (each repeated five times) were conditioned over saturated salt solutions, of known relative humidity, in an evacuated dessicator [5]. Samples were weighed before and after conditioning in order to deduce their moisture contents.

3.3. ESEM conditions

All experiments were carried out using an FEI Philips Electroscan ESEM, model 2010. An accelerating voltage of 10 kV was always used, and dry samples were imaged at room temperature and 4.5 torr chamber pressure. It was found that samples containing a predetermined moisture level could not withstand the initial optimised pumpdown sequence (mentioned earlier) within the specimen chamber, as this resulted in dehydration, and the crumbs were therefore hydrated *in situ* to replace lost moisture. *In situ* hydration was

achieved by lowering the sample temperature to ∼3°C while increasing the chamber pressure to 5.8 torr. A moisture content of around 16% can be obtained after approximately 19 minutes under these conditions, with 30% moisture content taking around 32 minutes to achieve. A series of control experiments, carried out at atmospheric pressure and ambient temperature outside the microscope, were used as a basis for comparing the stress-strain results obtained after *in situ* hydration, to give an indication of the moisture content attained by individual samples tested within the microscope.

4. Results and discussion

Breadcrumbs with a series of different moisture contents were compression tested using the tensile stage illustrated in Fig. 4. For this series, tests were not carried out within the chamber of the microscope, but rather at atmospheric pressure and ambient temperature. This enabled the general trends to be observed much more simply and accurately than would be possible with *in situ* testing (the results of *in situ* testing will be described and discussed later). The critical stress, determined from the maximum stress reached in each case, as a function of moisture content is shown in Fig. 5, while the critical strain as a function of moisture content is shown in Fig. 6. These graphs resemble the work of Attenburrow and co-workers [15] on the fracture behaviour of extruded wheat starch and gluten. In that work, the fracture stress/strain of gluten was small and showed no peak, but for wheat starch there was a significant increase in stress/strain at around 10% moisture. This figure is somewhat lower than our estimate of a peak at or near 16% moisture and may be due the nature and structure of the samples. Our work would appear to show that the mechanical response of breadcrumb, as a function of moisture content, follows the trend displayed by the extruded starch tested by Attenburrow *et al.*, rather than gluten. Other work on cellular cereal foods has also found that an intermediate degree of moisture is accompanied by a peak in the stress/strain at failure, confirming that stiffening occurs [6–8, 15, 16]. Sub-T_g mechanical relaxations (β relaxations) have been linked with plasticizer addition in polymers, leading to peaks in fracture resistance [17].

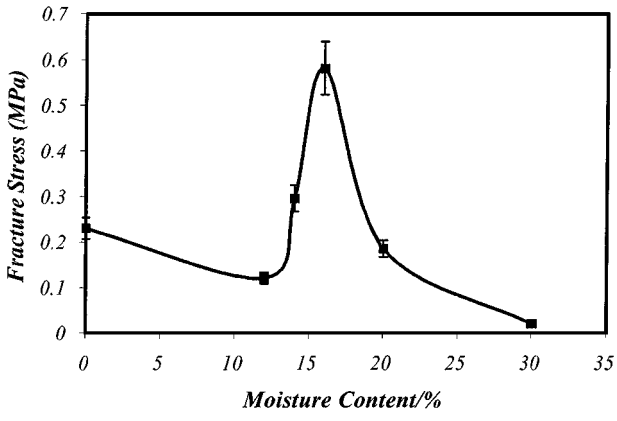

Figure 5 Plot of critical stress as a function of moisture content for breadcrumb.

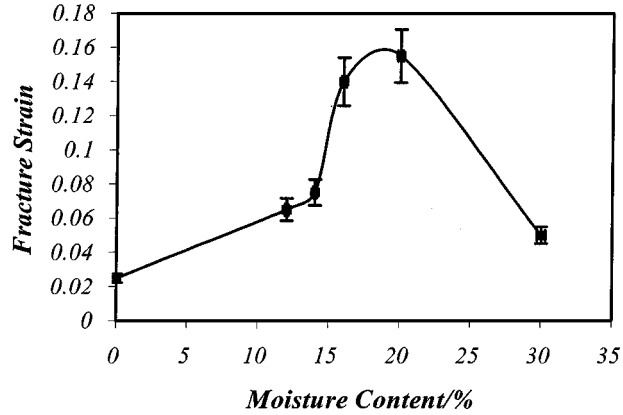

Figure 6 Plot of critical strain as a function of moisture content for breadcrumb.

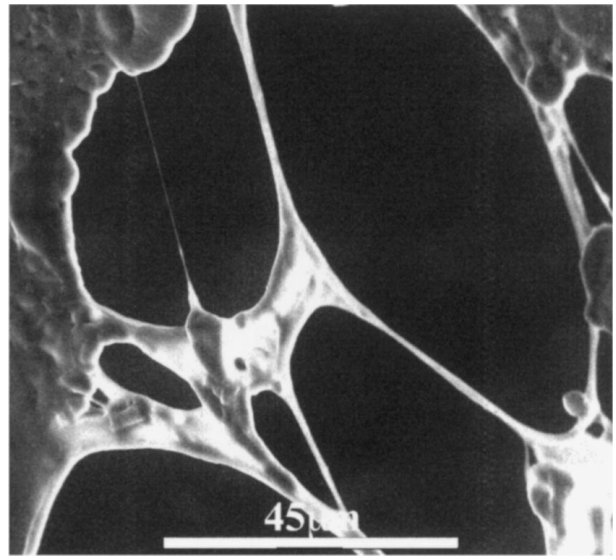

Figure 7 ESEM micrograph of 'strings' commonly observed in the microstructure of breadcrumb. These features stretch across the small voids found within cell walls.

Given that inherent flaws and defects act as stress concentrators [18], much of this work has been aimed at identifying such possible flaws and observing their behaviour under compressive stress, to understand their role in crumb fracture. A general feature of the breadcrumbs being used in this study is the presence of small 'voids' within cell walls, presumably formed as a consequence of escaping gases during baking. Stretching across these voids, images show evidence of bridging structures, potentially important for mechanical behaviour. An example is shown in Fig. 7, where fine 'strings' appear to span from one side of a void to another. Given the scale of such features, it is likely that they are mainly composed of gluten. Larger scale structures, here termed 'struts', have also been observed, often containing a small number of partially gelatinized starch granules.

4.1. Dry crumb

Compression testing of dry crumb samples produced consistent results, within experimental error, whether

the sample was tested using the straining stage outside the microscope or under ESEM conditions.

It can be seen, from the stress-strain curve in Fig. 8, that a low energy input is required for the initiation and propagation of fracture, indicative of brittle behaviour [19, 20], as is the jagged form of the plot [5]. Furthermore, dry samples tend to disintegrate at low strains (around 2%), due to their fragility, in agreement with other findings [5]. A demonstration of the overall failure mode of dry crumb is given in Fig. 9. The field of view is somewhat restricted in this particular ESEM, as the final pressure-limiting aperture is small, placing constraints on the area of sample scanned by the electron beam. Due to the relatively large scale of the crumb structure, this allows only a small section of the sample to be viewed. However, cell wall fracture can clearly be seen as a crack propagates through the structure, and this was observed to occur very rapidly. Close-up images taken during the compression testing of dry crumb are shown in Fig. 10, where the focus of attention is on structural flaws. The series of images in this figure clearly demonstrate that pre-existing discontinuities between starch granules and the gluten matrix are very likely to be weak points, and the presence of adjoining voids in the structure serves to concentrate the stress on these flaws. Together, these factors provide the source for a major failure mechanism at low strains. Furthermore, the failure propagates very quickly as the destroyed structure offers no resistance to further deformation. Fig. 11 shows another fracture surface in dry crumb, where intact starch granules are clearly visible, suggesting that the gluten matrix has yielded preferentially and de-cohesion has occurred.

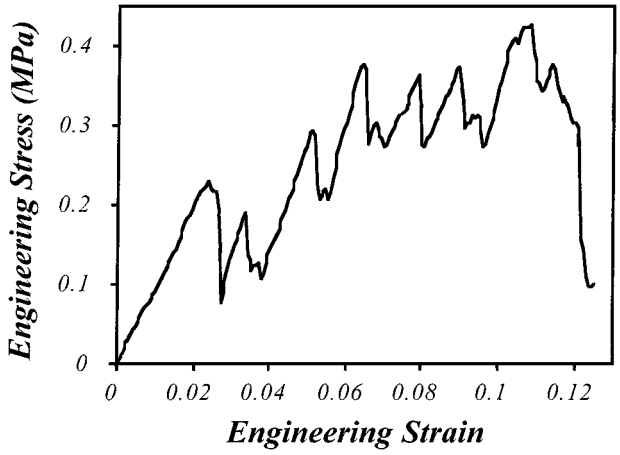

Figure 8 Stress-strain curve for the compression of dry breadcrumb. The onset of fracture occurs at very low strain (~2%). At around 12% strain, the sample disintegrates, indicative of brittle behaviour.

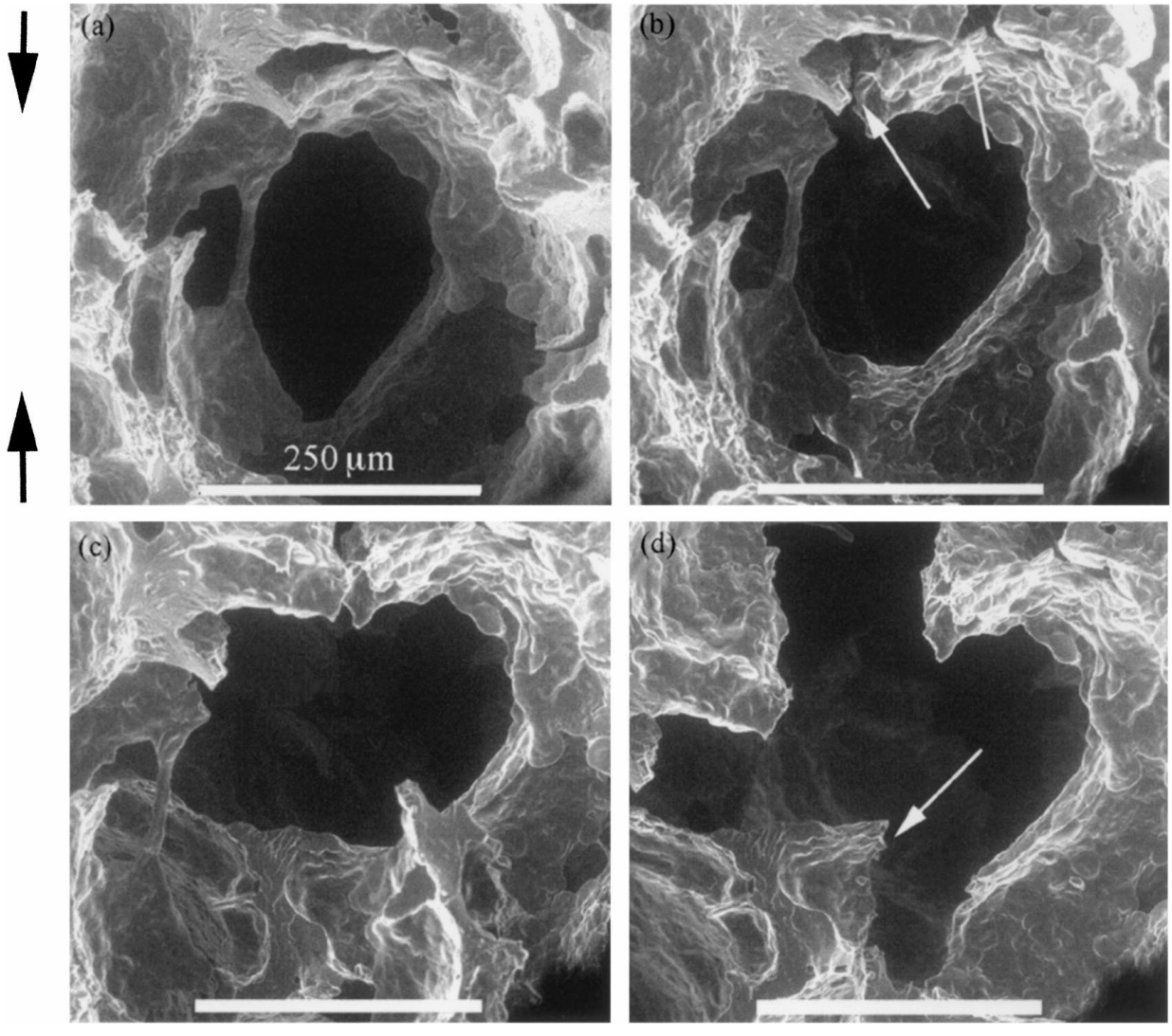

Figure 9 ESEM micrographs showing the general failure of cell walls in dry breadcrumb. Black arrows indicate the direction of applied strain.

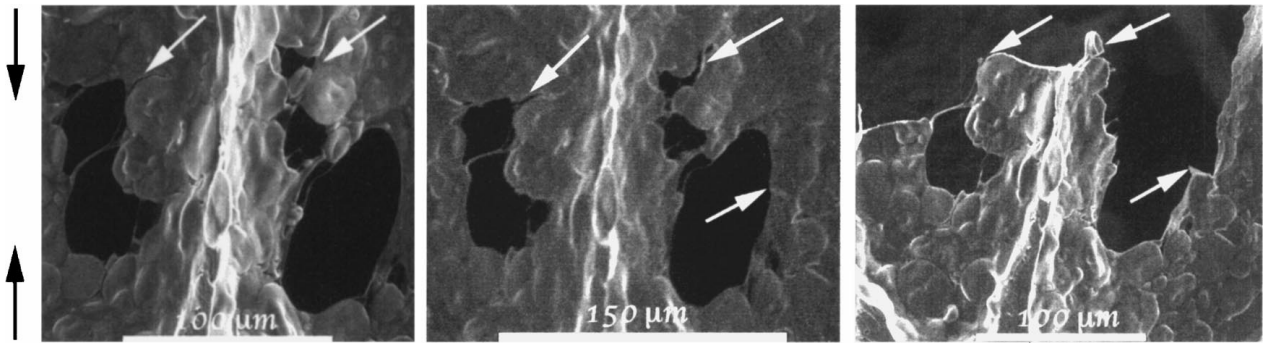

Figure 10 Close-up ESEM micrographs of cells in dry breadcrumb, with the cell wall running down the centre. Before testing (a), the sample has pre-existing voids in the starch-gluten matrix, along with regions where starch granules are incompletely adhered to the gluten (examples are marked with white arrows). As the sample is compressed (b), these apparent weak points in the structure begin to mobilize. The structure then yields along these flaws (c) as the brittle cell walls fracture rapidly and catastrophically. Black arrows show the direction of the applied strain.

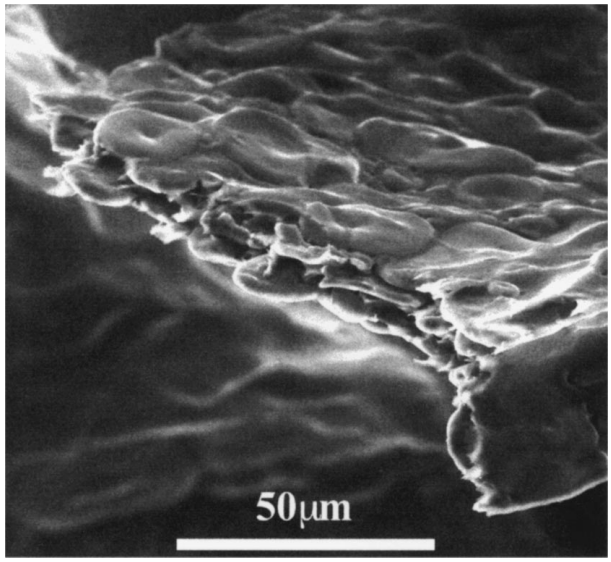

Figure 11 ESEM micrograph of another fracture surface elsewhere in the sample. The presence of intact starch granules along the leading edge of the fracture suggests that it is the gluten matrix that yields preferentially.

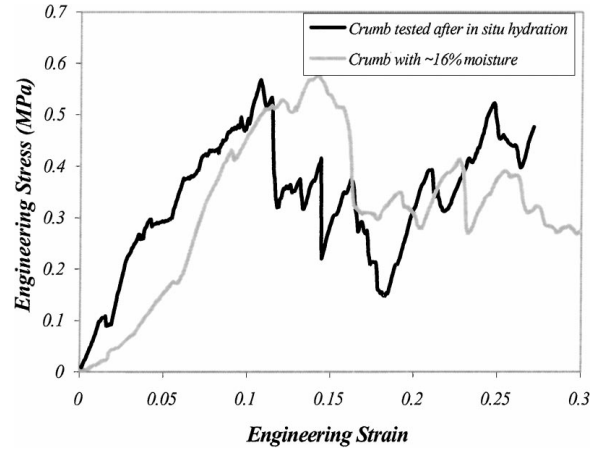

Figure 12 Stress-strain plot of crumb hydrated *in situ* for 19 minutes at 5.8 torr and 3°C, compared to that obtained for a crumb conditioned to 16% moisture content and tested under ambient conditions. The agreement between the two plots is very good, particularly in terms of their critical yield stresses.

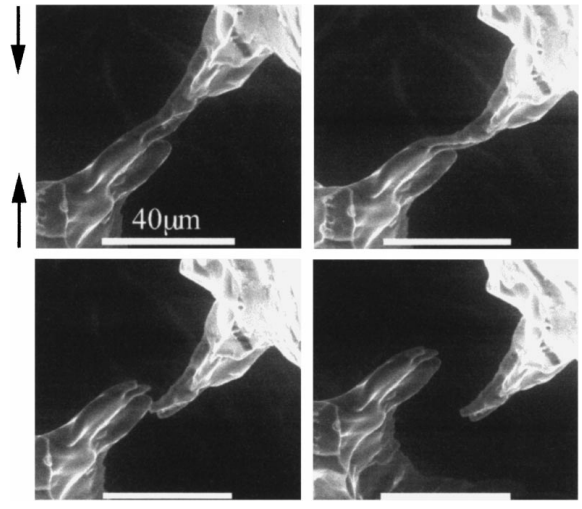

Figure 13 ESEM micrograph of crumb hydrated *in situ* to roughly 16% moisture content. The strut within a void in the cell wall deforms considerably before fracture occurs. Black arrows indicate the direction of applied strain.

4.2. Intermediate moisture crumb

Increasing the moisture content to ~16%, as Figs 12 and 13 demonstrate, causes a significant change in the behaviour of the breadcrumb. As noted earlier, it was found that crumb samples with pre-determined moisture contents appeared to suffer dehydration during the pump-down procedure of the ESEM, despite due care to prevent this. The result was a significant lack of correlation between the stress/strain behaviour of like samples, and so a method of *in situ* hydration was developed as described in the experimental section. To this end, the stress-strain curves in Fig. 12 serve as a comparison between a typical compression test conducted outside the microscope on a pre-conditioned crumb sample, and a similar crumb sample hydrated and tested *in situ*. Given the random nature of testing crumb samples, the plots are in good agreement, and suggest that the method is successful. In terms of the mechanical behaviour of such intermediate moisture crumb samples, the plots reveal a steep rise in the stress before the onset of failure. The pronounced drop in stress immediately after the critical stress is reached suggests that the crumb has become ductile [19] or is undergoing plastic yielding [21]. It has been suggested that at moderate moisture levels such as this, the structural matrix is only partially plasticised and that this makes the structure more cohesive and less prone to disintegration [5]. During *in situ*

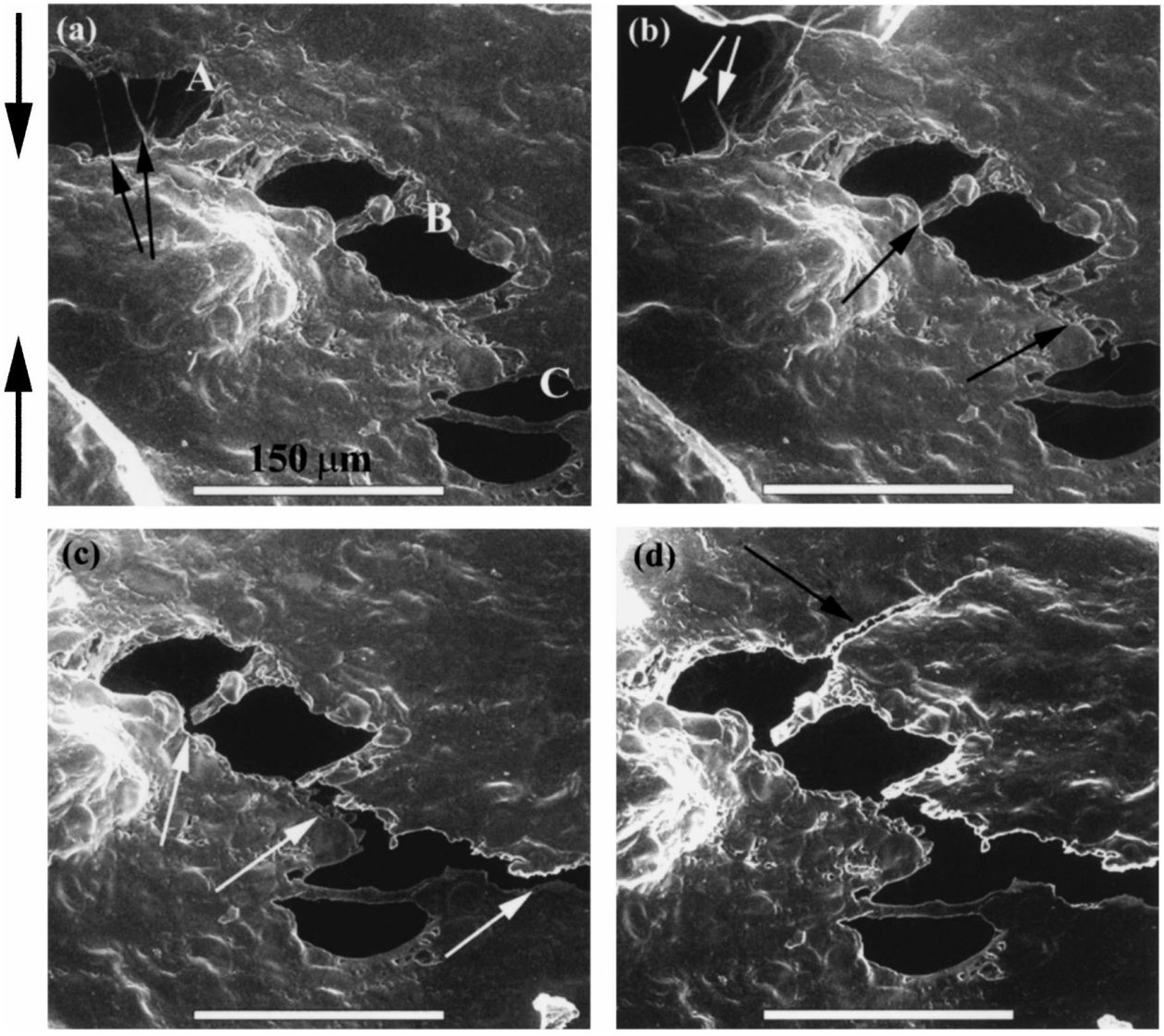

Figure 14 ESEM micrographs of another crumb hydrated *in situ* to 16% moisture content. See text for discussion.

compression testing of intermediate moisture samples, the rate of fracture initiation and propagation was visibly slower than in the dry crumb samples. This is borne out in Fig. 12 where the strain at maximum deformation is roughly 15%, compared to only 2% for dry samples. The strut shown in Fig. 13 appears to exhibit ductile behaviour, as it is seen to distort significantly, before eventually failing. It is possible that struts such as this provide resistance to the propagation of cracks, at intermediate moisture, by absorbing energy and thereby increasing the mechanical strength of the crumb, perhaps leading to stiffening. A further facet of the deformation of intermediate moisture crumb is shown in Fig. 14, and again, attention has been focused on several voids within the cell wall. In 14a, void A is bridged by strings in a direction parallel to the applied strain, while voids B and C are bridged by struts. The strut in void C is in a direction perpendicular to the applied stress. At a small strain, 14b, void A has failed and the accompanying strings have snapped. A crack has also begun to propagate from right-to-left, and has weakened the region between voids B and C. The perpendicular orientation of the strut in void C confers little or no additional strength, and the crack propagates, as shown in 14c. As

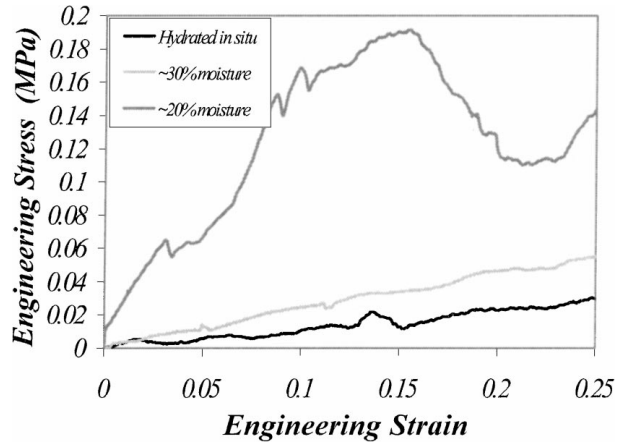

Figure 15 Stress-strain plot for a crumb sample hydrated *in situ* to approximately 30% moisture content. The stiffness of the sample has dramatically decreased, as evidenced by the very shallow curve. The results of testing pre-conditioned crumbs, under ambient conditions, are also shown for comparison.

the crack propagates, it is evident that the stress is concentrated on the strut in void B, causing it to fracture at the base. This seems to deflect the path of the crack, as a new crack emerges at the top of the strut, shown in 14d.

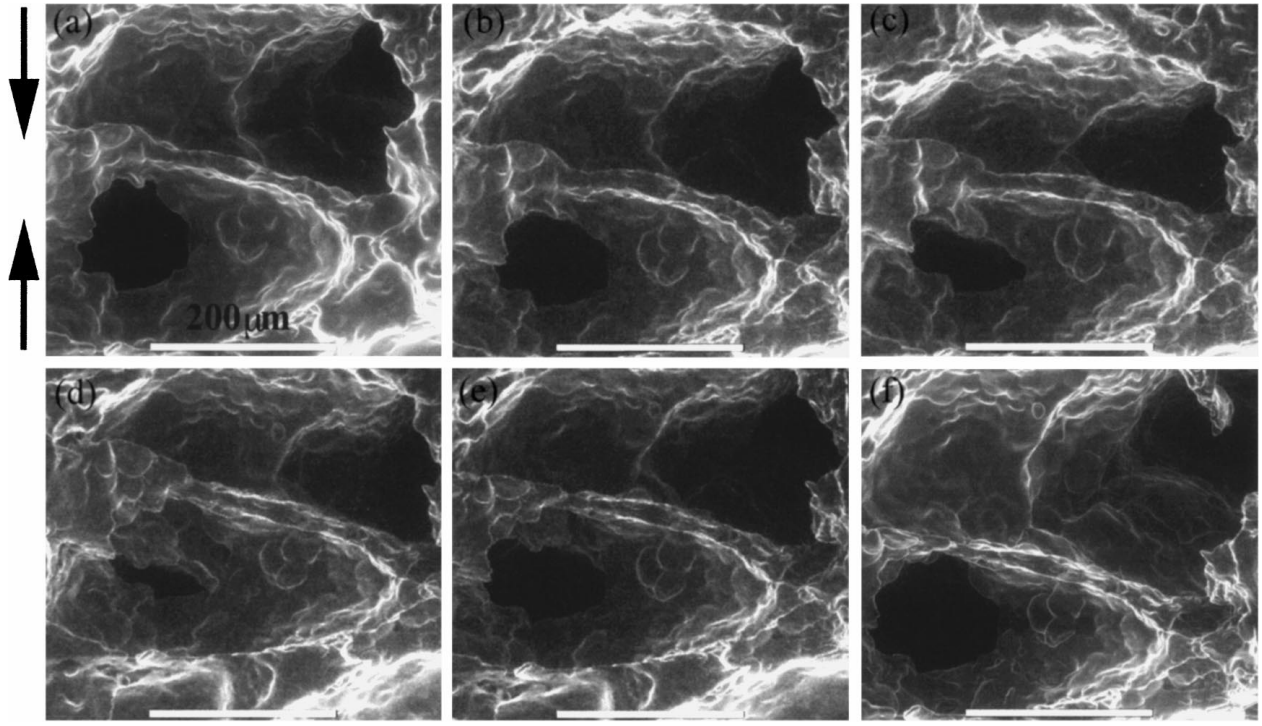

Figure 16 ESEM micrographs of crumb at approximately 30% moisture content (based on data obtained from samples at 30% moisture content that were tested outside the microscope). The sample has been subjected to a cyclic test, and it is possible to see how the cell featured is able to buckle elastically, (a)–(d), and then recover the applied strain upon its removal, (e)–(f). Black arrows indicate the direction of the strain applied in (a)–(d).

4.3. High moisture crumb

A stress-strain plot representing the behaviour of high moisture crumb, arbitrarily taken to be 30% or higher in these experiments, is shown in Fig. 15. Again, the crumb has been hydrated and tested *in situ*, as described in the experimental section. The result is compared with the outcome of tests on crumb samples that have been pre-conditioned to approximately 20% and 30% moisture contents, and then compression tested under ambient conditions. It is clear that the crumb hydrated *in situ* behaves in a similar manner to the crumb with 30% moisture. From the stress-strain plots it can be seen that, at high moisture content, the crumb is highly plasticised. Such behaviour has been likened [6] to the effect of plasticisers on synthetic polymers, in which plasticiser molecules screen off attractive forces between polymer chains and/or enlarge the spaces between polymer chains, allowing chain segments greater freedom of movement [22, 23]. This plasticisation is manifested as a decrease in the glass transition temperature T_g [24]. The compression-decompression cycle shown in Fig. 16 demonstrates the elastomeric behaviour that is to be expected of such a sample. The cell wall buckles elastically during compression and, upon removal of the applied stress, all of the strain is recovered as the cell wall resumes essentially its original shape. Finally, Fig. 17 follows the mechanical response of struts in a crumb of roughly 30% moisture. After a small strain, the strut marked in the figure has begun to bend, 17b, and by 17c this is even more noticable as the cell walls on either side of the void begin to close in on each other. In 17d there is dramatic change in the strut's response, as it begins to buckle in the opposite direction to that in which it was previously bending. It is also apparent that

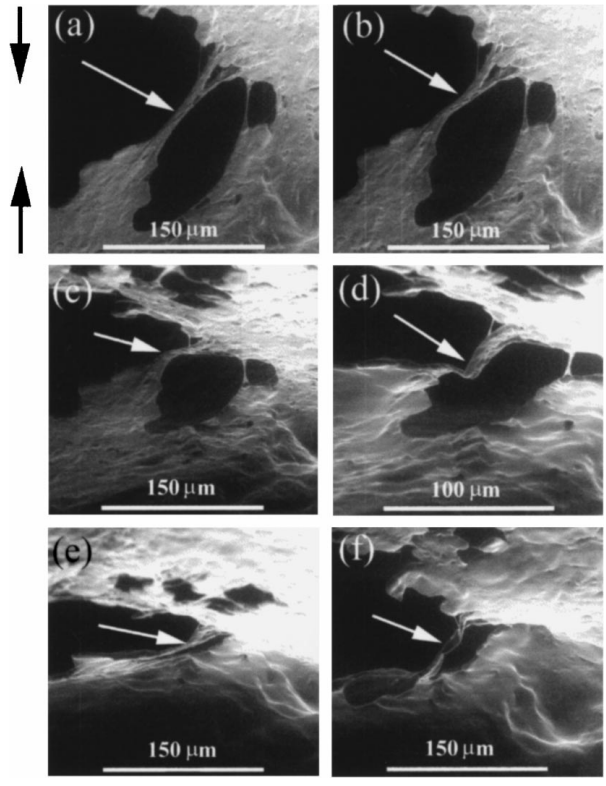

Figure 17 ESEM micrographs showing the behaviour of struts at high moisture content.

the outlines of starch granules on the surface of the sample, visible in 17a–c, are obscured as water is squeezed from the matrix. The strut continues to distort, without fracturing, until it begins to touch a neighbouring part of the void, 17e. Upon removal of the applied stress,

17f, the strut begins to recover, although the structure has been rather disrupted by excess water and so complete recovery is not observed in this region. It is clear that the strut did not fracture, even at very high strain, although there was some evidence of cell wall failure in other parts of the sample.

5. Conclusions

A method has been developed whereby quantitative stress-strain data has been obtained for breadcrumb, at different levels of hydration, coupled with simultaneous imaging of failure mechanisms within the ESEM. Samples can be imaged in their natural state, requiring none of the standard preparation techniques such as the freezing/drying and metallic coating needed in conventional SEM. The ESEM provides good depth of field, and allows bulk samples to be tested. This technique offers a potential means for investigating the effects of mechanical testing on a wide range of materials, enabling us to study the ways in which these materials respond in real-time, dynamic experiments.

We have found that the compressive stress and strain responses of breadcrumb, both dry and hydrated, are in general agreement with previous work, in that a maximum in these quantities occurs at intermediate moisture content.

Dry samples display brittle, fragile characteristics indicative of the glassy state. The results of this study suggest that the starch/gluten interface plays a significant role in determining failure initiation in breadcrumb. We have observed that interfaces between starch granules and the gluten matrix, sometimes in the presence of voids in cell walls, serve to provide a source for the concentration of stress fields and hence fracture initiation/propagation. ESEM images reveal preferential yielding of the gluten matrix, leaving behind intact starch granules at the interface.

A brittle-to-ductile transition appears to occur at intermediate moisture. The stress before fracture increases significantly, consistent with, for example, partial plasticisation of the matrix, increasing the structural cohesion and conferring greater mechanical strength to the material as a whole. We have seen that voids in cell walls are often bridged by small-scale features such as fine strings and larger struts. The ESEM images that we have presented suggest that these features play an important role in affecting the propagation of cracks, particularly at intermediate moisture content. Struts were seen to distort before fracture, absorbing energy and potentially increasing the stiffness of the crumb. The orientation of strings and struts, relative to the direction of applied stress, may also be a determining factor in the propagation of cracks.

High moisture samples are in a rubbery state, presumably well above their T_g, giving the expected elastomeric properties. ESEM images confirm that the majority of cell walls bend elastically, recovering much of their original shape upon removal of the applied strain, although some failure does occur.

This innovative technique has therefore been used for a revealing study of breadcrumbs. It is hoped that ESEM will become a valuable complementary tool for the investigation of the mechanical properties of many different materials, particularly those not previously accessible by electron microscopy.

Acknowledgements

The authors wish to thank Dr B.L. Thiel and Mr P. Bone for their assistance. Funding for this work was provided by BBSRC and Du Pont (UK) Ltd., Cereals Innovation Centre, Cambridge, England.

References

1. H. MCGEE, "On Food and Cooking. The Science and Lore of the Kitchen." (Harper Collins, 1991).
2. T. SHUKLA, *Cereal Foods World* **38**(9) (1993) 701–702.
3. L. A. KUNTZ, *Food Product Design.* (April) (1997) 39–56.
4. R. F. SCHIFFMANN, in "The Technology of Microwavable Coated Foods, in Batters and Breadings in Food Processing," edited by K. Kulp and R. Loewe (AACC, St. Paul, MN, 1990) p. 153–162.
5. M. HARRIS and M. PELEG, *Cereal Chemistry* **73**(2) (1996) 225–231.
6. G. ATTENBURROW and A. P. DAVIES, in "The Glassy State in Foods," edited by J. M. V. Blanshard and P. J. Lillford (Nottingham University Press, 1993) p. 317–331.
7. I. FONTANET, S. DAUIDOU, C. DACREMONT and M. LE MESTE, *J. Cereal Science.* **25** (1997) 303–311.
8. G. ROUDAUT, C. DACREMONT and M. LE MESTE, *Journal of Texture Studies* **29** (1998) 199–213.
9. ELECTROSCAN, Electroscan Model 2010 Manual, 66, Concord Street, Wilmington, MA 01887, USA, 1994.
10. R. CAMERON and A. DONALD, *J. Microscopy* **173**(3) (1994) 227–237.
11. R. DURKIN and J. S. SHAH, *ibid.* **169** (1993) 33–51.
12. B. THIEL *et al.*, *ibid.* **187**(Pt. 3) (1997) 143–157.
13. A. FLETCHER, B. THIEL and A. DONALD, *J. Phys. D: Appl. Phys.* **30** (1997) 2249–2257.
14. M. PELEG, *Food Science and Technology International* **3** (1997) 227–240.
15. G. E. ATTENBURROW *et al.*, *Journal of Cereal Science* **16** (1992) 1–12.
16. R. J. NICHOLLS *et al.*, *ibid.* **21** (1995) 25–36.
17. L. E. NIELSEN, "Mechanical Properties of Polymers and Composites" (Marcel Dekker, New York, 1994) Chap. 4.
18. R. W. DAVIDGE, "Cambridge Solid State Science Series" (Cambridge University Press, Cambridge, 1974).
19. F. C. CHANG, J. S. WU and L. H. CHU, *Journal of Applied Polymer Science* **44** (1992) 491–504.
20. J. VINCENT, "Structural Biomaterials (Revised Edition)" (Princeton, Princeton University Press, New Jersey, 1990).
21. L. GIBSON and M. ASHBY, "Cellular Solids. Structure and Properties" (Pergammon Press, 1998).
22. T. ALFREY, "Mechanical Behaviour of High Polymers" (Interscience, 1948).
23. N. A. J. PLATZER, *Advances in Chemistry Series,* **48** (1965) 23–28.
24. L. SLADE and H. LEVINE, in "The Glassy State in Foods," edited by J. M. V. Blanshard and P. J. Lillford (Nottingham University Press, Loughborough, Leics., 1993) p. 35–101.

Received 20 January
and accepted 22 July 1999